Wireless Intra-Body Power Transfer via Capacitively Coupled Link

Noor Mohammed

Electrical and Computer Engineering University of Massachusetts Amherst MA, USA

noormohammed@umass.edu

Robert W. Jackson

Electrical and Computer Engineering University of Massachusetts Amherst MA, USA

jackson@ecs.umass.edu

Jeremy Gummeson

Electrical and Computer Engineering

University of Massachusetts Amherst
MA, USA

igummeso@umass.edu

Sunghoon Ivan Lee

College of Information & Computer Science
University of Massachusetts Amherst
MA, USA
silee@cs.umass.edu

Abstract—Over the past couple of years, the Capacitive Intra-Body Power Transfer (C-IBPT) technology, which uses the human body as a wireless power transfer medium via capacitive links, has received tremendous attention in the field as a potential solution to support a network of battery-free body sensors. However, circuit modeling of C-IBPT systems, despite its importance in supporting the reliable operation of battery-free body sensors, has been significantly understudied in the field. This paper proposes a finite element model (FEM) and equivalent linear circuit models to estimate path loss and inter-electrode capacitance of a C-IBPT system. As a demonstrative example, the model approximates a typical human forearm (from wrist to elbow) and allows for investigation of the transmission loss between a skin-coupled power transmitter and a receiver in the electro-quasistatic domain. The computed transmission loss from the proposed model is further validated against experimental measurements obtained from five healthy human subjects using a wearable 40~MHz radio frequency (RF) transmitter and an isolated power receiver system in a laboratory environment. The preliminary experimental data show an approximate $40 \ dB$ transmission loss within $10 \ cm$ body channel length for the parallel plate electrode configuration with dimensions of $30~mm \times 40~mm$. The simulation finding shows a lower transmission loss of 35 dB and 13.5 fF coupling capacitance across a 10 cm body channel.

Index Terms—Intra-body power transfer, Capacitive power transfer, Wireless power transfer, RF Energy Harvester.

I. INTRODUCTION

Recent advancements in ultra-low-power sensors and CMOS devices have supported the development of novel wearable applications for fitness and health monitoring [1]. This paves the way for next-generation body sensor networks consisting of tens of on-body devices [2], [3]. However, powering a network of devices across the human body without disrupting their continuous operation remains a particular challenge since batteries require frequent recharging and replacement due to their finite number of charge cycles [1]. Therefore, intermittent computing to support battery-free devices has been

This work is supported in part by the NSF under Grant No. 016419-00001.

a paramount topic of research in the field of body sensor networks.

Many strategies have been proposed in the literature to support battery-free, wireless on-body devices. For example, direct wiring between battery-free devices and a power source via a textile link can be realized under special clothing arrangements [4]. However, this approach requires the users to wear an additional garment to operate wearable devices, which may impart burden to the user and is not suitable for long-term and continuous health monitoring. Wireless transfer of power to battery-free devices via inductive links or far-field electromagnetic (EM) wave propagation has also received tremendous attention [5]. Nevertheless, these approaches are vulnerable to line-of-sight misalignment and body shadowing effects, hampering the reliable operation of the devices.

To support a network of battery-free body sensors, researchers have investigated the use of the human body as a wireless power transfer medium via capacitive links [1], namely the Capacitive Intra-Body Power Transfer (C-IBPT) technology. C-IBPT technologies have the potential to support a network of battery-free body sensors whose power could be managed by a single on-body power source. However, despite its potential, C-IBPT is still in its early stage of research and development. In a typical C-IBPT setting, the human body offers a direct, conductive forward path for low radio frequency (RF) energy within the tens of MHz range with a return path established via a weak parasitic capacitive coupling between two ground (metal) plates of the transmitter and receivers. Circuit modeling is an important first step toward improving our understanding of the C-IBPT transmission loop. We refer to the paper by Shukla et al. [6] for a more detailed overview of the C-IBPT technology.

In this work, we investigate a C-IBPT system using the human forearm as a demonstrative power transfer channel. We compare the transmission losses attained via 3D FEM and equivalent two-port linear circuit simulations vs. experimental measurements obtained from five healthy subjects. We also

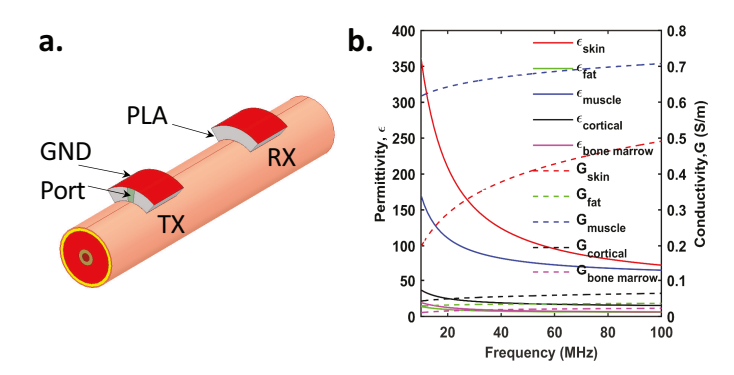


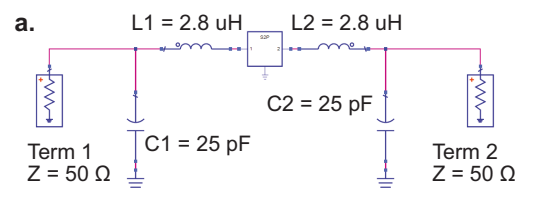
Fig. 1. 3D FEM Model of the capacitive link. Here, (a) hand FEM model showing detailed view of the tissue layers, and (b) frequency dependence of different tissue properties used in the proposed FEM model.

provide an estimation of the return path coupling capacitance between a pair of ground plates over the $10\ cm$ human body (forearm) channel.

II. BIOPHYSICAL MODEL

Several studies have reported different methodologies and models that describe electric field propagation through the human body, which is largely motivated by a research area called Human Body Communication (HBC). HBC leverages the human body as a communication medium between two battery-powered on-body devices, which could also be coupled capacitively (i.e., C-HBC) [7]. Prior research has investigated the theoretical modeling of electrodes as electric dipoles over finite conductive planes [8], lumped RC modeling of electrodes and the body channel [9], 3D FEM of multilayered body tissue [1], and circuit-coupled 3D FEM of the C-HBC system [7]. However, each of them exhibits specific differences and limitations that isolate C-IBPT from C-HBC on several occasions. For example, the conventional HBC introduces a common ground, which is defined as a hypothetical earth/instrument ground that establishes capacitive coupling to the transmitting and receiving electrodes' ground to construct the return path [7], [9], [10]. One of the main objectives of these studies was to enhance the coupling capacitance between this common ground and the electrodes' ground. However, the need for an external physical ground is omitted in the proposed C-IBPT technique to promote more ubiquitous applications. In C-IBPT, the main design objective is to enhance the coupling capacitance between the electrodes' ground instead of including an additional conductive plane to complement the virtual ground. As a result, we assume that the dominant current loop will be established via capacitive coupling between the local electrodes' ground without requiring any exterior physical ground.

This manuscript proposes a unifying hybrid model that includes a frequency-dependent multilayered 3D FEM model of the human body—more specifically, the human forearm—with a fixed wearable electrode system. The FEM simulation provides the two-port scattering parameters. These scattering



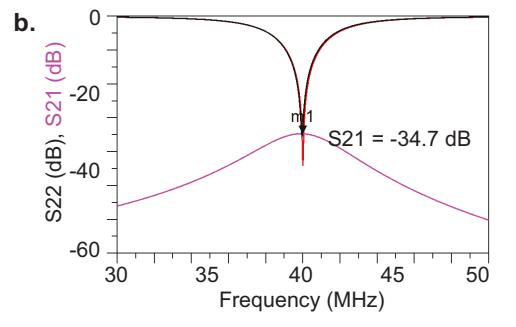


Fig. 2. (a) The equivalent circuit model of the 3D FEM model with matching networks. (b) Resultant S-parameters showing the transmission gain of $-34.7\ dB$.

parameters are used to create a two-port linear circuit model that can be used to analyze the transmission gain.

A. 3D FEM Model

Fig. 1(a) illustrates the proposed 3D FEM model of a human forearm. This cylindrical model consisted of layers of skin (0.75 mm), fat (2.6 mm), muscle (15.65 mm), cortical bone (3.4 mm), and bone marrow (3.6 mm) with a total radius of $26 \ mm$ and a length of $300 \ mm$. The specific values of tissue thicknesses were obtained from a prior study [11]. Each tissue layer was modeled with frequencydependent conductivity and permittivity based on the FCC database on human tissue properties [12], as shown in Fig. 1(b). The transmitting and receiving electrodes were identical, comprising a rectangular skin electrode and a ground plate configuration (30 $mm \times 40 \ mm$ in size). The electrodes were gold-plated copper with a thickness of 35 μm , which was higher than the skin depth of copper at 40 MHz. The dielectric substrate between the electrodes contained a very low permittivity material (i.e., PLA plastic with an average permittivity of 3.1) with a thickness of 11 mm. The low permittivity property of the substrate reduces the capacitive coupling between the skin and ground electrodes, increasing the terminal potential difference across the electrodes. The radiation boundary was modeled as a 500 cm air cube to enable the absorbing boundary conditions. The entire system was solved for the 50 Ω two-port S-parameters using the full wave electromagnetic solver of ANSYS HFSS Software. The computation provides a 2-port S-matrix model, which is used to compute the gain at matched conditions (i.e., -34.7 dB), as illustrated in Fig. 2.

B. Circuit Model

Fig. 3 shows an equivalent circuit that models the results of the 3D FEM model. In this model, the electrodes' impedance

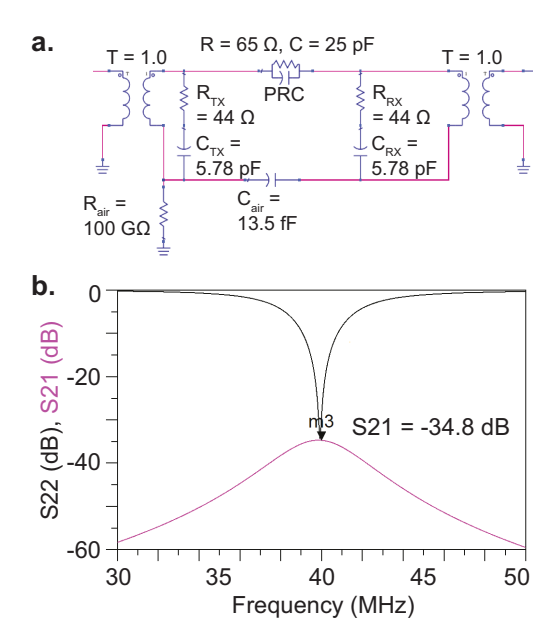


Fig. 3. (a) The equivalent circuit model of the C-IBPT system to determine inter-electrode capacitance. (b) Resultant S-parameters obtained from the circuit model showing the transmission gain of $-34.8\ dB$.

values ($R_{TX} = R_{RX}, C_{TX} = C_{RX}$) were obtained from the S-matrix at 40~MHz provided by the FEM simulation. The R and C components in the PRC element represent lumped RC components for a tissue in the forearm. The values of these lumped components were obtained from a prior study [10], which we assumed are independent of the electrode configuration. Two ideal baluns with no interwinding capacitance were introduced to isolate the air return path from the common ground. The ADS simulation requires a DC return path in the isolated loop, which was created by adding an extremely high resistance (i.e., $R_{air} = 100~G\Omega$). Fig. 3(b) shows the S_{21} response from the circuit model with matching network from Fig. 2. The return path capacitance C_{air} was tuned to 13.5~fF to obtain a transmission gain that matches the $|S_{21}|$ of the FEM simulation.

Based on the circuit model in Fig. 3, a simple approximate expression for the gain can be determined. The Y-parameters for the model in Fig. 3 are $Y_{11}\simeq (R_{TX}+1/j\omega C_{TX})^{-1}$ and $Y_{21}\simeq 1/j\omega C_{air}$, where the impedance of C_{air} is assumed to be much greater than that of the electrode (R_{TX},C_{TX}) or of the body (R,C). The maximum available gain can be determined from $G_{MAG}=K(1-\sqrt{1-1/K^2})$, where $K=[2Re(Y_{11})^2-Re(Y_{21}^2)]/|Y_{21}|^2$ for a symmetric circuit. An assumption that $\omega C_{TX}R_{TX}<<1$ resulted in $K\simeq 2(C_{TX}/C_{air})^2\omega^2C_{TX}^2R_{TX}^2$, which was much greater than 1 for the parameters in this configuration. This yielded

$$G_{MAG} \simeq \left(\frac{C_{air}}{C_{TX}}\right)^2 \cdot \frac{1}{(2\omega C_{TX}R_{TX})^2} = \left(\frac{C_{air}}{C_{TX}}\right)^2 \cdot Q_{TX}^2,$$

where Q_{TX} is the Q of the electrode circuit. For the circuit model in Fig. 3, we set $Q_{TX}=7.8$ and $C_{air}/C_{TX}=2.3\times 10^{-3}$. Using these values, the equation (1) produces a gain

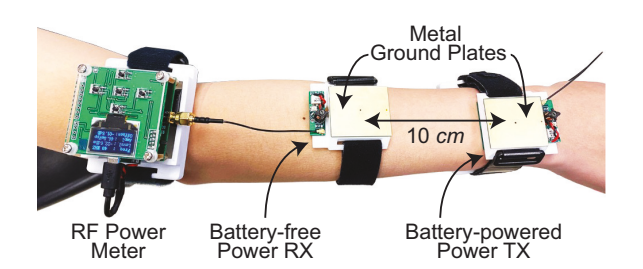


Fig. 4. Experimental setup to measure the path loss between transmitting and receiving electrodes.

TABLE I
EXPERIMENTAL RESULTS SHOWING THE RECEIVED POWER AND GAIN
OBTAINED FROM FIVE HEALTHY HUMAN SUBJECTS.

Subject	P_{TX} (dBm)	P_{RX} (dBm)	Gain (dB)
1	18.5	-21.1	-39.6
2	18.5	-22.6	-41.1
3	18.5	-21.9	-40.4
4	18.5	-21.2	-39.7
5	18.5	-22.6	-41.1
Overall	18.5	-21.9 ± 0.7	-40.4 ± 0.7

of $-35 \ dB$, which is in good agreement with the simulated results shown in Figs. 2 and 3. This equation demonstrates how high electrode Q can enhance the matched circuit gain.

III. EXPERIMENTAL SETUP AND RESULTS

Fig. 4 illustrates the experimental setup to verify the gain obtained from the equivalent circuit of the FEM model. This block was connected to battery-operated, $50~\Omega$ -matched wearable RF power transmitter and receiver, as shown in Fig. 3. Both transmitter and receiver are attached to skin-coupled electrodes. Each of the electrodes consists of one practical balun with interwinding capacitance [13]. Note that we adopted single port measurement during impedance data collection of the skin coupled electrode. In addition, we introduced an additional balun between the VNA port and the electrode to isolate the resonance artifact contributed by the benchtop VNA ground. Finally, during transmission gain data collection, a handheld VNA (Nano VNA) was used to tune the electrode across subjects to maintain a constant impedance match (i.e., $-40~dB~S_{11}$).

Fig. 5(a) shows the implemented matching networks, and Fig. 5(b) shows the measured S_{11} data obtained from this matching network. Note that the experimental LC matching networks have the shunt capacitance across the balun instead of the $50~\Omega$ source side. This is the consequence of additional parasitic capacitance contributed by the practical balun with other passive components, such as capacitors and inductors with finite Q, and PCB implementation of the circuits. As a result, we designed a matching network that can absorb the additional parasitic capacitance while maintaining the $50~\Omega$ matched condition.

Table I summarizes the received signal strength (P_{RX}) and gain observed from five healthy human subjects. The

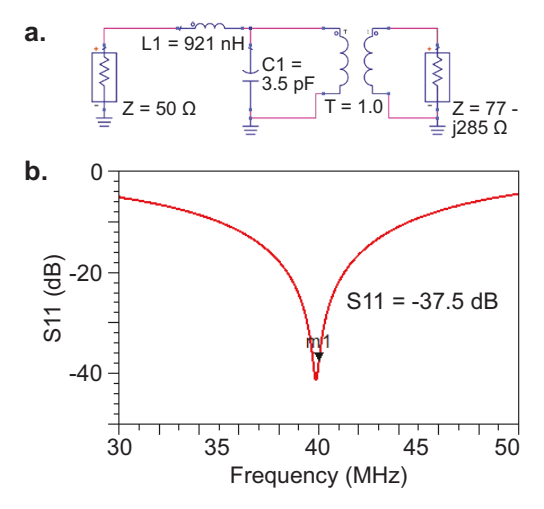


Fig. 5. (a) Designed matching network for the skin coupled electrode having an impedance of $77 - j285 \Omega$ at $40 \ MHz$. (b) S_{11} response obtained from the matched skin coupled electrode during single port measurement.

experiments were conducted in a typical lab environment having a relative humidity of $50\pm3\%$ and temperature of $20\pm2^{\circ}C$. The transmitted signal strength (P_{TX}) was 18.5~dBm for all subjects, whereas the received signal strength was $-21.9\pm0.7~dBm$ across the five subjects at 10~cm forearm body channel length. Consequently, the resultant transmission gain was $-40.4\pm0.7~dB$.

IV. DISCUSSION

From the proposed C-IBPT circuit models, the transmission gain is a vital function of the electrode size, matching quality, and coupling capacitance. On the other hand, the impedance offered by the body tissue (i.e., the forward path) has less influence on the transmission gain because it results in minimal contributions to the loop impedance. The simulation indicates that the return path capacitance is the limiting factor in determining the overall transmission gain. Again, the return path capacitance is primarily influenced by the separation distance between the transmitter and receiver's ground electrode. Therefore, the optimum return path capacitance could be achieved by defining a suitable channel length, the maximum coverage area for a specific transmitter, and the ground electrode sizes. The body shadowing effect can also affect the return path capacitance, which remains an essential component of future work. The reported results showed a 5.7 dB difference between the simulated and empirically measured gains (i.e., 40.4 vs. 34.7 dB), which could result from resistive losses within the matching network [14] and the practical baluns. Additionally, the proposed FEM model represents a truncated part of the human body. In contrast, the empirical data are obtained from full-sized humans, which might also contribute to the discrepancies between the simulated and the observed data.

V. CONCLUSION

This work has introduced a 3D FEM model and equivalent circuit model to numerically investigate the C-IBPT transmis-

sion gain and return path capacitance for a fixed 40~MHz RF signal at a 10~cm body channel length. The simulation and experimental results show an approximate transmission gain of -35~dB to -40~dB for a simulated coupling capacitance of 13.5~fF between a $30~mm \times 40~mm$ skin-coupled electrode pair at a 10~cm body channel length. Finally, the proposed computational model described in this paper has allowed us to study the feasibility and design challenges of a C-IBPT system using both S-matrix and RC coupled models. Hence, future work will leverage this model to design an optimized electrode system for efficient power transmission in a C-IBPT system.

REFERENCES

- [1] N. Mohammed, R. Wang, R. W. Jackson, Y. Noh, J. Gummeson, and S. I. Lee, "Shazam: Charge-free wearable devices via intra-body power transfer from everyday objects," *Proceedings of the ACM on Interactive, Mobile, Wearable and Ubiquitous Technologies*, vol. 5, no. 2, pp. 1–25, 2021.
- [2] S. Han, J. Kim, S. M. Won, Y. Ma, D. Kang, Z. Xie, K.-T. Lee, H. U. Chung, A. Banks, S. Min et al., "Battery-free, wireless sensors for full-body pressure and temperature mapping," *Science translational medicine*, vol. 10, no. 435, p. eaan4950, 2018.
- [3] D.-H. Kim, N. Lu, R. Ma, Y.-S. Kim, R.-H. Kim, S. Wang, J. Wu, S. M. Won, H. Tao, A. Islam *et al.*, "Epidermal electronics," *science*, vol. 333, no. 6044, pp. 838–843, 2011.
- [4] R. Takahashi, W. Yukita, T. Sasatani, T. Yokota, T. Someya, and Y. Kawahara, "Twin meander coil: Sensitive readout of battery-free onbody wireless sensors using body-scale meander coils," *Proceedings of* the ACM on Interactive, Mobile, Wearable and Ubiquitous Technologies, vol. 5, no. 4, pp. 1–21, 2021.
- [5] A. P. Sample, D. J. Yeager, P. S. Powledge, A. V. Mamishev, and J. R. Smith, "Design of an rfid-based battery-free programmable sensing platform," *IEEE transactions on instrumentation and measurement*, vol. 57, no. 11, pp. 2608–2615, 2008.
- [6] R. Shukla, N. Kiran, R. Wang, J. Gummeson, and S. I. Lee, "Skinny-power: enabling batteryless wearable sensors via intra-body power transfer," in *Proceedings of the 17th Conference on Embedded Networked Sensor Systems*, 2019, pp. 68–82.
- [7] A. Datta, M. Nath, D. Yang, and S. Sen, "Advanced biophysical model to capture channel variability for eqs capacitive hbc," *IEEE Transactions* on *Biomedical Engineering*, vol. 68, no. 11, pp. 3435–3446, 2021.
- [8] J. Bae, H. Cho, K. Song, H. Lee, and H.-J. Yoo, "The signal transmission mechanism on the surface of human body for body channel communication," *IEEE Transactions on microwave theory and techniques*, vol. 60, no. 3, pp. 582–593, 2012.
- [9] J. Park, H. Garudadri, and P. P. Mercier, "Channel modeling of miniaturized battery-powered capacitive human body communication systems," *IEEE Transactions on Biomedical Engineering*, vol. 64, no. 2, pp. 452–462, 2016.
- [10] M. D. Pereira, G. A. Alvarez-Botero, and F. R. de Sousa, "Characterization and modeling of the capacitive hbc channel," *IEEE Transactions on Instrumentation and Measurement*, vol. 64, no. 10, pp. 2626–2635, 2015.
- [11] J. Mao, H. Yang, Y. Lian, and B. Zhao, "A self-adaptive capacitive compensation technique for body channel communication," *IEEE Trans*actions on Biomedical Circuits and Systems, vol. 11, no. 5, pp. 1001– 1012, 2017.
- [12] "Body tissue dielectric parameters," Sep 2020. [Online]. Available: https://www.fcc.gov/general/body-tissue-dielectric-parameters
- [13] J. Sakai, L.-S. Wu, H.-C. Sun, and Y.-X. Guo, "Balun's effect on the measurement of transmission characteristics for intrabody communication channel," in 2013 IEEE MTT-S International Microwave Workshop Series on RF and Wireless Technologies for Biomedical and Healthcare Applications (IMWS-BIO). IEEE, 2013, pp. 1–3.
- [14] E. Wen, D. Sievenpiper, and P. P. Mercier, "Channel characterization of magnetic human body communication," *IEEE Transactions on Biomed*ical Engineering, 2021.